

Mixing at mid-ocean ridges controlled by small-scale convection and plate motion

Henri Samuel^{1,2,3*} and Scott D. King^{3,4}

Oceanic lavas are thought to be derived from different sources within the Earth's mantle, each with a distinct composition^{1–4}. Large-scale plate motions provide the primary mechanism for mixing these sources, yet the geochemical signature of lavas erupted at different mid-ocean ridges can still vary significantly^{5,6}. Geochemical variability is low where plate spreading rates are high, consistent with plate-scale mixing^{5,6}. However, slow-spreading centres, such as the Southwest Indian Ridge in the Indian Ocean, are also geochemically homogeneous, which is inconsistent with plate-scale mixing^{6,7}. Here we use numerical simulations of mantle flow to study mantle mixing at mid-ocean ridges, under conditions with variable plate length and spreading rate. Our simulations reveal that small-scale convection in the mantle contributes significantly to mantle mixing at slow spreading rates; faster plate velocities and smaller plates inhibit small-scale convection. We conclude that whereas fast-spreading ridge lavas are well mixed by plate-scale flow, slow-spreading ridge lavas are mixed by small-scale convection.

From a fluid dynamics point of view, surface plate motion is directly linked to underlying mantle deformation and mixing^{8–10}. However, mantle dynamics is more than plate-scale flow; thermal instabilities progressively develop below lithospheric plates, leading to small-scale convective motions. Such instabilities are theoretically predicted¹¹ and observed in numerical simulations^{12–16} and laboratory experiments^{17,18}. In addition, small-scale convective motion is consistent with the asymptotic behaviour of oceanic heat flow, geoid, and bathymetry at old plate ages¹⁹. However, the influence of small-scale convection on mantle convective mixing has not been quantified, and is only marginally considered in the interpretation of the geochemical data at mid-ocean ridges²⁰.

We conducted a series of numerical mantle convection experiments in a rectangular domain with imposed surface ridge motions (see Supplementary Information 1 for numerical modelling details). We systematically varied the two governing parameters: the dimensionless distance between the ridge axis and the edge of the domain between one and three times the depth of the domain ($H = 1–3$), and the magnitude of the dimensionless plate velocity between 0 and 35 cm yr^{-1} (represented by a dimensionless Péclet number, $Pe = 0–16,000$). For each computation, we measure the efficiency of convective mixing by computing the positive finite-time Lyapunov exponents (FTLEs), λ^+ , which provide a measure of the Lagrangian strain rate. Large values of λ^+ indicate a well-mixed region, and small values of λ^+ indicate a less-well mixed, or more heterogeneous, region (see Supplementary Information 2 for details about the computation of FTLEs).

At small plate velocities, convection is vigorous and well developed with upwelling plumes originating from the base of the

mantle (Fig. 1a). Two types of downwelling are observed: two large-scale, cold slabs subducting at the edges of the domain owing to the imposed velocity field, and small-scale convection triggered by the destabilization of the sublithospheric thermal boundary layer^{17,18}. The superposition of multiple scales of convection with high temporal variability leads to a homogeneous (Fig. 1g), Gaussian distribution of the FTLEs (Fig. 1m) with large average values; indicating that the fluid is well mixed. With increasing plate velocity, we observed a significant decrease in the FTLEs, indicating that the fluid is progressively more heterogeneous (Fig. 1h and n). This inverse relationship between ridge spreading rate and degree of mixing contradicts the standard assumption made when interpreting isotopic variability among mid-ocean ridge basalt (MORB) samples. Moreover, beyond a threshold for the plate velocity close to 4 cm yr^{-1} (Fig. 1d), we observe a pronounced change in mantle mixing processes. For ridge spreading rates above the critical value ($Pe > Pe_c$) small-scale convection is completely absent and mantle flow becomes governed only by large-scale surface plate motions (Fig. 1d–f) with weaker time dependence (Fig. 2a).

The disappearance of small-scale, strongly time-dependent, convection with increasing plate velocity reduces the regions of intense deformation to only a few fixed hyperbolic points⁸ located at convergent margins (for example, the upper edges of the convective domain), or divergent margins (for example, the ridge axis). In these regions, mixing efficiency remains chaotic (that is, the Lagrangian strain exhibits an exponential time dependence, see Fig. 1j–l) and keeps on increasing with increasing plate velocity. Elsewhere, the flow is dominated by rotation (it is said to be elliptic) with weak simple-shear-like deformation (Fig. 1j–l). Hence, the degree of mixing in these elliptic regions is regular (that is, weak) as indicated by the small FTLE values (that is, the Lagrangian strain exhibits a linear time dependence).

The coexistence of regular and chaotic mixing regions within a highly viscous convecting system has been previously identified in plate-driven flows⁹, and was attributed to the presence of a toroidal component of motion (that is, horizontal shear). The calculations here have no toroidal component of flow yet generate a similar spatially heterogeneous pattern in the degree of mixing. The transition from mixed small-scale convection with large-scale flow to purely plate-driven motion shifts the corresponding distribution of FTLE values from a single peak (Fig. 1m–o), to multiple peaks (Fig. 1p–r). This leads to a V-shaped curve of the root mean squared values of FTLE associated with an increase in the strength of spatial heterogeneity in mixing efficiency with increasing plate velocity (Fig. 2b). Additional experiments carried out at lower ($H = 1$) and higher ($H = 3$) values of the domain aspect ratio (Fig. 2c) and for other viscous rheologies (Supplementary Section 3) confirm that

¹CNRS, IRAP, 14, avenue Edouard Belin, F-31400 Toulouse, France, ²Université de Toulouse, UPS-OMP, IRAP, F-31400 Toulouse, France, ³Bayerisches Geoinstitut, Universität Bayreuth, D-95447, Germany, ⁴Virginia Tech, Blacksburg, Virginia 24060, USA. *e-mail: henri.samuel@irap.omp.eu

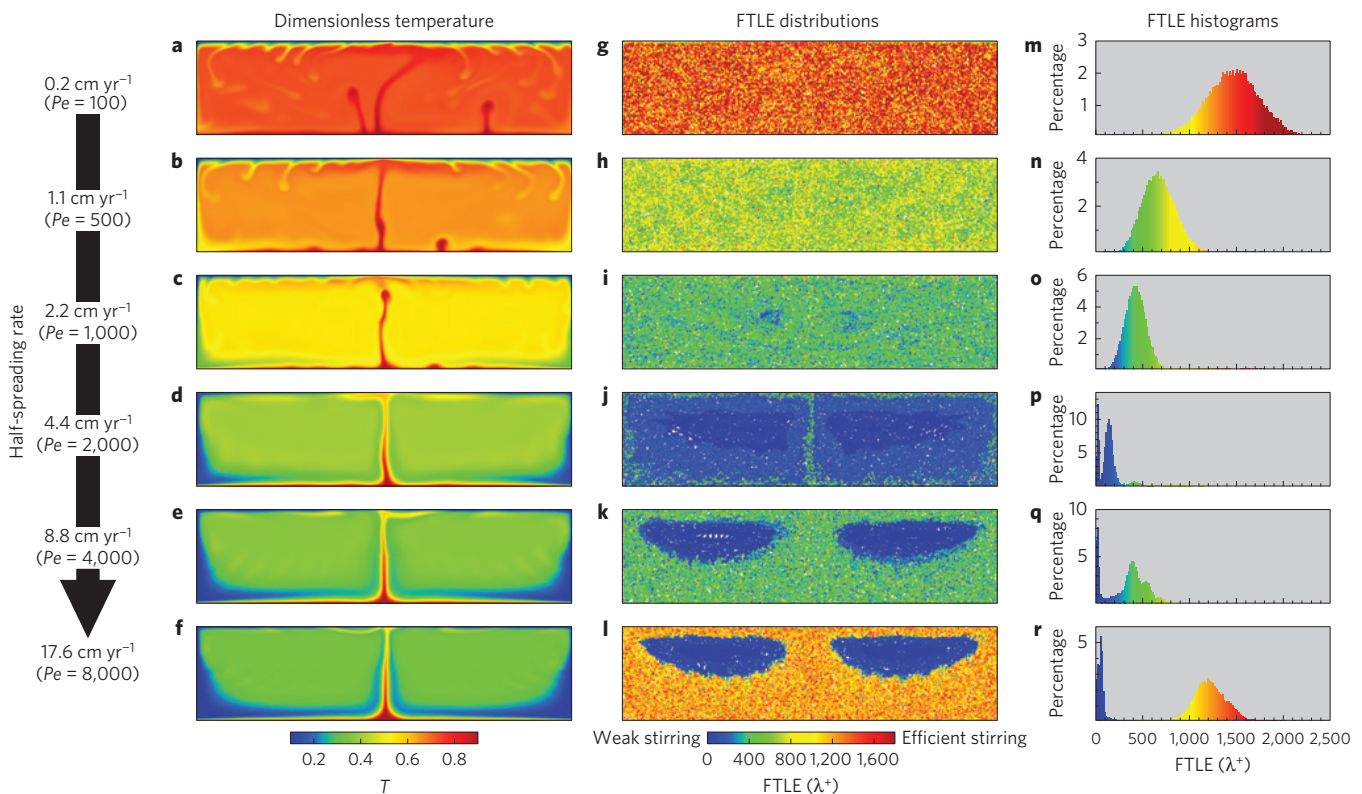


Figure 1 | Numerical experiment results: temperature fields and mixing efficiencies for cases with different half-spreading rates. The entire mantle depth ($D=2,900 \times 10^3$ m) is shown, and $H=2$ (that is, the width of the domain is $2HD$). **a–f**, Dimensionless potential temperature fields. **g–l**, FTLE distributions. **m–r**, FTLE histograms.

the V-shaped curves shown in Fig. 2 for the temporal variations of convective velocities and the spatial variations of Lyapunov exponents are robust features.

The critical value of plate velocity, Pe_c , (that is, the bottom of the 'V') that marks the transition between the mixed convective regime and the large-scale flow is a function of the domain aspect ratio, H (Supplementary Section 4). Although our models are two-dimensional, they capture the main dynamics of mantle mixing in the context of mid-ocean ridges. Indeed, in three-dimensional space, the main mechanisms for small-scale convection (for example, onset time, convective velocities) and plate-driven flow are comparable^{9,15,16}. Moreover, the relationship between stirring processes and convective velocities in highly viscous fluid flow (the case of the Earth's mantle) remains similar²¹ in three dimensions.

Making the reasonable assumption that the isotopic variability of basalt samples is directly related to the degree of mantle convective mixing (or to the degree of heterogeneity of mantle sources), several implications can be drawn from our results. First, the standard assumption that the degree of mixing increases with convective velocities is correct only in the vicinity of the ridge axis or within bands along the edges of the convective domain, and is valid only for fast ridge spreading rates (in the sense that $Pe > Pe_c$). For relatively slow ridge spreading rates ($Pe < Pe_c$), the influence of small-scale convection decreases with increasing plate velocity, leading to a progressive decrease in mixing efficiency, contrary to the standard assumption^{5,6}. Second, the mantle is well mixed at slow-spreading ridge regions, something the standard assumption can not explain. Third, the mantle is very heterogeneous at fast spreading ridges and the degree of mixing increases on average with the spreading rate. However, the well-mixed region is limited to the vicinity of the ridge axis or close the edges of the convective domain, and the rest of the domain (of significant extent) is characterized by regions

that are less-well mixed and independent of the ridge spreading rate (Fig. 1j–l).

Our results have important implications for the interpretation of isotopic MORB and ocean island basalt (OIB) samples. To illustrate this we have performed comparative predictions of the isotopic variability of MORB samples in the main mid-ocean ridge systems segmented into eight regions (superimposed on the oceanic seafloor ages from ref. 22, see Fig. 3a, Supplementary Table 1 and Supplementary Section 4 for details about the calculations of mixing times). The MORB isotopic variability in these regions is illustrated by the standard deviation of helium data and this is shown in Fig. 3b. In the first prediction, we made the standard assumption that MORB isotopic variability is inversely proportional to the ridge spreading rate (pink circles in Fig. 3c). As discussed previously, these predictions are inconsistent with the observed small isotopic variability of MORB samples along the Southwest Indian Ridge^{6,7} (SWIR; Fig. 3a,b). In the second prediction (blue stars in Fig. 3c), on the basis of insight from our experiments, we make the assumption that MORB variability is also related to the extent of oceanic small-scale convection (hence, to the maximum seafloor age within each region), and therefore may increase with decreasing the ridge spreading rate. The comparison of the pink trend shown in Fig. 3c with the trend from the data shown in Fig. 3b shows a poor agreement between the data trend and the predicted trend that accounts only for large-scale flow. In contrast, there is a good match between the data trend and the predicted trend that accounts for small-scale convection (blue dotted curve).

To further facilitate the comparison with the data shown in Fig. 3b, one can relate the mixing times shown in Fig. 3c with the standard deviation of chemical heterogeneities, under the reasonable assumption of chaotic mixing (see Supplementary Information 4 for a discussion of the underlying assumptions and

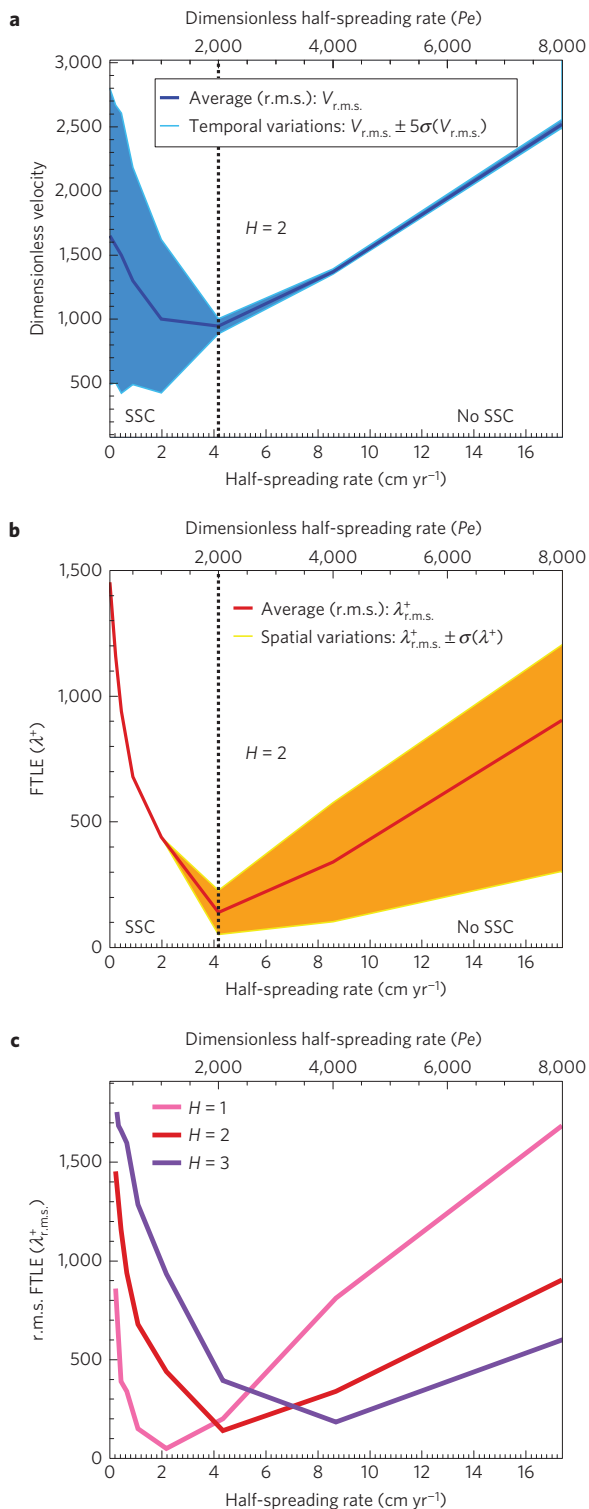


Figure 2 | Numerical experiment results: averaged quantities and variability versus half-spreading rate. **a**, Root mean squared convective velocity ($V_{r.m.s.}$) averaged over several mantle overturns (dark blue curve) and temporal variability of $V_{r.m.s.}$ (light blue areas: five times the standard deviation value). **b**, Root mean squared FTLEs ($\lambda_{r.m.s.}^+$) averaged over the whole domain (red curve) and spatial variability of $\lambda_{r.m.s.}^+$ (orange areas) taken as half the difference between the two main peaks in the FTLE distribution (that is, it measures the deviation from a mono-modal, Gaussian distribution). Dashed lines in **a** and **b** separate regions where small-scale convection (SSC) is present from regions without small-scale convection (No SSC). **c**, Root mean squared FTLE values for various H .

details on the calculations). Figure 3d shows the corresponding predicted standard deviations. The linearly decreasing standard deviations obtained when considering that mixing at ridges results from purely plate-driven flow fails to explain the data. However, when considering both small-scale convection and plate-driven flow, the obtained trend compares well to the data. The differences in predicted mixing times and variability between the blue and pink curves (Fig. 3c,d) at both slow (SWIR, Mid-Atlantic Ridge (MAR)) and fast ridges (East Pacific Rise (EPR)) are due to the presence of small-scale convection. Despite its fast spreading rate, small-scale length of the convection is well established for the EPR owing to the length of the Pacific plate, allowing for small-scale convection to develop even at the fastest spreading rates. The predicted differences in isotopic variability among ridges can be obtained only within only the past 200 Myr of evolution during which the plate configuration remains approximately steady.

The assumption that MORB variability is related to the extent of oceanic small-scale convection resolves the apparent inconsistency for the ultraslow-spreading SWIR, whose samples exhibit remarkably small isotopic variability (Fig. 3b). Furthermore, our results suggest that the coexistence of regular and chaotic regions explains several characteristic differences in the variance between MORB and OIB isotopic compositions. Indeed, in the large-scale regime, the mixing is very efficient in the vicinity of the ridge axis where MORB material is sampled. However, in regions that are away from the axis the degree of mixing can drop by orders of magnitude. If these weakly mixed regions are sampled by upwelling mantle plumes that generate OIB material, they would produce highly variable isotopic compositions. Only a small fraction of this highly heterogeneous material sampled by plumes would significantly enhance the variability of resulting isotopic signatures. This mechanism does not univocally preclude the existence of other isolated geochemical mantle reservoirs in various forms^{23–28}. However, it can explain characteristic differences between MORB and OIB isotopic variability and composition^{1–4}.

Received 11 February 2014; accepted 20 June 2014; published online 20 July 2014

References

- Allègre, C. J., Moreira, M. & Staudacher, T. ⁴He/³He dispersion and mantle convection. *Geophys. Res. Lett.* **22**, 2325–2326 (1995).
- Hofmann, A. W. Mantle geochemistry: The message from oceanic volcanism. *Nature* **385**, 219–229 (1997).
- Farley, K. A. & Neroda, E. Noble gases in the Earth's mantle. *Ann. Rev. Earth Planet. Sci. Lett.* **26**, 189–218 (1998).
- Ballentine, C. J., van Keken, P. E., Porcelli, D. & Hauri, E. H. Numerical models, geochemistry and the zero-paradox noble-gas mantle. *Phil. Trans. R. Soc. Lond. A* **360**, 2611–2631 (2002).
- Allègre, C. J., Hamelin, B. & Dupré, B. Statistical analysis of isotopic ratios in MORB: The mantle blob cluster model and the convective regime of the mantle. *Earth Planet. Sci. Lett.* **71**, 71–84 (1984).
- Graham, D. W. in *Noble Gases in Geochemistry and Cosmochemistry* (eds Wieler, R., Porcelli, D. & Ballentine, C. J.) 243–319 (2002).
- Georgen, E. J., Kurz, M. D., Dick, H. J. B. & Lin, J. Low ⁴He/⁴He ratios in basalt glasses from the western Southwest Indian Ridge (10°–24°E). *Earth Planet. Sci. Lett.* **206**, 509–528 (2003).
- Ottino, J. M. *The Kinematics of Mixing: Stretching, Chaos and Transport* (Cambridge Univ. Press, 1989).
- Ferrachat, S. & Ricard, Y. Regular vs. chaotic mantle mixing. *Earth Planet. Sci. Lett.* **155**, 75–86 (1998).
- Van Keken, P. E. & Zhong, S. Mixing in a 3D spherical model of present-day mantle convection. *Earth Planet. Sci. Lett.* **171**, 533–547 (1999).
- Landuyt, W. & Ierley, G. Linear stability analysis of the onset of sublithospheric convection. *Geophys. J. Int.* **189**, 19–28 (2012).
- King, S. D. & Anderson, D. L. Edge driven convection. *Earth Planet. Sci. Lett.* **160**, 289–296 (1998).
- King, S. D. & Ritsema, J. African hot spot volcanism: Small-scale convection beneath cratons. *Science* **290**, 1137–1140 (2000).

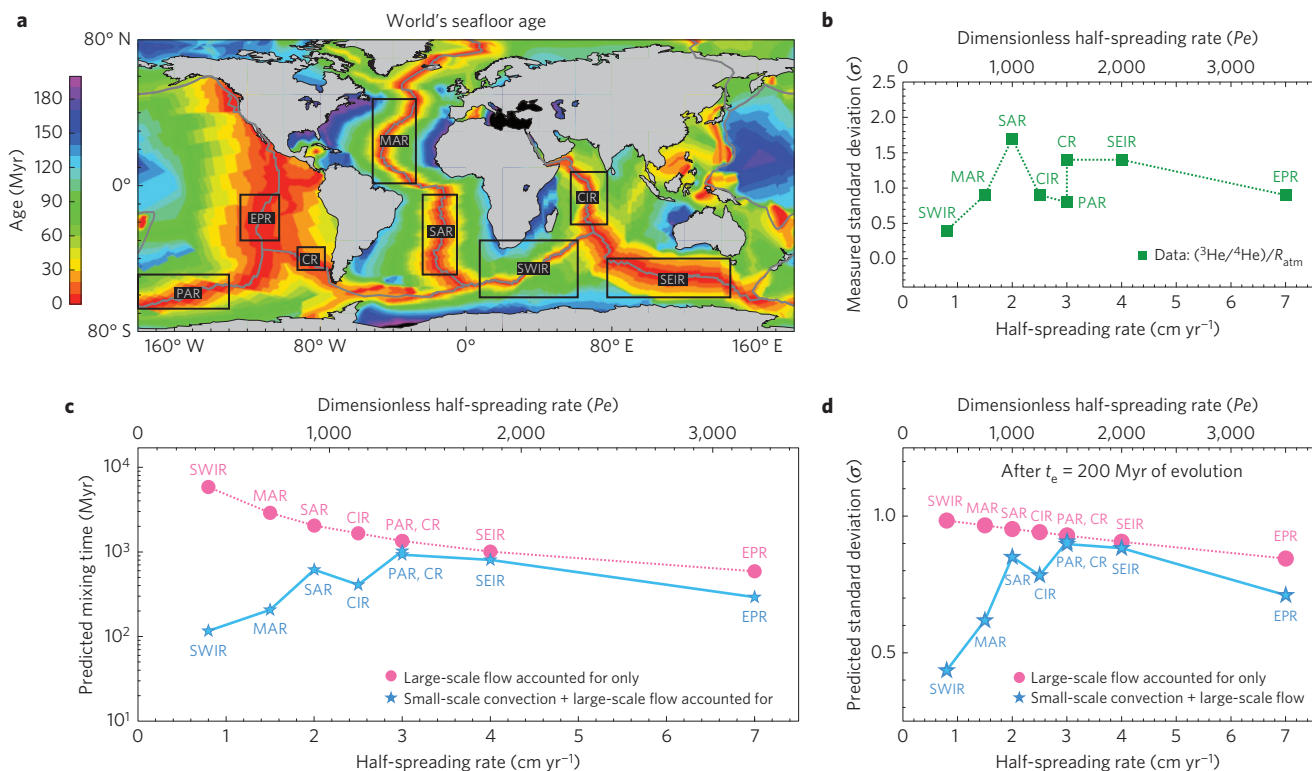


Figure 3 | Helium variability and predicted mixing times along mid-ocean ridges. **a**, Seafloor age and eight selected regions (labelled rectangles) considered in **b–d**. **b**, Standard deviation of $R = {}^3\text{He}/{}^4\text{He}$ measured along spreading centres, normalized to the atmospheric ratio value, R_{atm} , versus ridge's half-spreading rate. **c,d**, Predicted mixing times (**c**) and standard deviations (**d**) of chemical heterogeneities versus ridge's half-spreading rate, assuming that mixing is entirely due to surface-plate motion (pink circles), or making the more reasonable assumption that mixing results from the combination of small-scale convection and surface-plate motion (blue stars). See Supplementary Sections 4 and 5 for further details. PAR, Pacific-Antarctic Ridge; EPR, East Pacific Rise; CR, Chile Ridge; MAR, Mid-Atlantic Ridge; SAR, South Atlantic Ridge; SWIR, Southwest Indian Ridge; CIR, Central Indian Ridge; SEIR, Southeast Indian Ridge.

- Dumoulin, C., Doin, M.-P. & Fleitout, L. Numerical simulation of the cooling of an oceanic lithosphere above a convective mantle. *Earth Planet. Sci. Lett.* **125**, 45–64 (2001).
- Van Hunen, J., Huang, J. & Zhong, S. The effect of shearing on the onset and vigor of small-scale convection in a Newtonian rheology. *Geophys. Res. Lett.* **30**, 1991 (2003).
- Ballmer, M. D., Ito, G., van Hunen, J., Bianco, T. A. & Tackley, P. J. Small-scale sublithospheric convection reconciles geochemistry and geochronology of 'Superplume' volcanism in the western and south Pacific. *Earth Planet. Sci. Lett.* **290**, 40–54 (2010).
- Parsons, B. & McKenzie, D. P. Mantle convection and the thermal structure of the plates. *J. Geophys. Res.* **83**, 4485–4496 (1978).
- Davaille, A. & Jaupart, C. Onset of thermal convection in fluids with temperature-dependent viscosity: Application to the oceanic mantle. *J. Geophys. Res.* **99**, 19853–19866 (1994).
- Stein, C. A. & Stein, S. A model for the global variation in oceanic depth and heat flow with lithospheric age. *Nature* **359**, 123–129 (1992).
- Graham, D. W., Lupton, J. E., Spera, F. J. & Christie, D. M. Upper-mantle dynamics revealed by helium isotope variations along the Southeast Indian ridge. *Nature* **409**, 701–703 (2001).
- Coltice, N. & Schmalz, J. Mixing times in the mantle of the early Earth derived from 2-D and 3-D numerical simulations of convection. *Geophys. Res. Lett.* **33**, L23304 (2006).
- Müller, D. R., Sdrolias, M., Gaina, C. & Roest, W. R. Age, spreading rates, and spreading asymmetry of the world's ocean crust. *Geochem. Geophys. Res.* **9**, Q04006 (2008).
- Manga, M. Mixing of chemical heterogeneities in the mantle: Effect of viscosity differences. *Geophys. Res. Lett.* **23**, 403–406 (1996).
- Albarède, F. & van der Hilst, R. D. On the nature and scale of mantle convection. *Eos* **80**, 535–539 (1999).
- Samuel, H. & Farnetani, C. G. Thermochemical convection and helium concentrations in mantle plumes. *Earth Planet. Sci. Lett.* **207**, 39–56 (2003).
- Samuel, H., Farnetani, C. G. & Andrault, D. in *Structure Composition and Evolution of the Earth's Mantle* (eds Bass, J., van der Hilst, R. D., Matas, J. & Tampert, J.) 100–116 (American Geophysical Union, 2005).
- Boyett, M. & Carlson, R. W. ${}^{142}\text{Nd}$ evidence for early (>4.53 Ga) global differentiation of the silicate Earth. *Science* **309**, 576–581 (2005).
- Li, M., McNamara, A. K. & Garnero, E. J. Chemical complexity of hotspots caused by cycling oceanic crust through mantle reservoirs. *Nature Geosci.* **7**, 366–370 (2014).

Acknowledgements

This work benefited from comments by D. Graham. H.S. acknowledges the funds from the Deutsche Forschungsgemeinschaft (project SA 2042/2-1), from the Stifterverband für die Deutsche Wissenschaft, and from the Centre de Coopération Universitaire Franco-Bavarois. S.D.K. acknowledges the funds from the Humboldt Foundation. Figures were made with the Generic Mapping Tools (P. Wessel and W.H.F. Smith, EOS, Trans. AGU 76 (1995) 329).

Author contributions

H.S. and S.D.K. conceived the study and designed the experiments. H.S. performed the experiments, analysed the data and developed the semi-analytic mixing model. H.S. and S.D.K. discussed the results and wrote the text.

Additional information

Supplementary information is available in the online version of the paper. Reprints and permissions information is available online at www.nature.com/reprints. Correspondence and requests for materials should be addressed to H.S.

Competing financial interests

The authors declare no competing financial interests.